

# Wavelet Packets for Fast Solution of Electromagnetic Integral Equations

Wojciech L. Golik

**Abstract**—This paper considers the problem of wavelet sparsification of matrices arising in numerical solution of electromagnetic integral equations by the method of moments. Scattering of plane waves from two-dimensional (2-D) cylinders is computed numerically using a constant number of test functions per wavelength. Discrete wavelet packet (DWP) similarity transformations and thresholding are applied to system matrices to obtain sparsity. If thresholds are selected to keep relative residual error constant the matrix sparsity is of order  $O(N^p)$  with  $p < 2$ . This stands in contrast with  $O(N^2)$  sparsities obtained with standard wavelet transformations [1]. Numerical tests also show that the DWP method yields faster matrix–vector multiplication than some fast multipole algorithms.

**Index Terms**—Moment methods, wavelet transforms.

## I. INTRODUCTION

NUMERICAL solutions for electromagnetic integral equations describing scattering from electrically large complex objects continues to be a challenging problem. The classical method of moments produces dense linear systems with  $N$  unknowns, where  $N$  grows with the electrical size of the scattering object. Since any direct solvers for dense systems have  $O(N^3)$  complexity, they become impractical for large  $N$  and iterative methods must be used. The cost of one iteration for such methods is dominated by a matrix–vector multiplication (MVM), the complexity of which is proportional to the number of nonzero matrix elements.

In recent years, various approaches have been proposed to decrease the complexity of MVM's in numerical solution of electromagnetic integral equations. In general, two avenues for development of fast MVM's are available: algorithms that bypass the complete construction of the impedance matrix and algorithms relying on matrix transformations. Among the former is the fast multipole method (FMM) [2], [3] and the adaptive integral method (AIM) [4]. The latter approaches include the impedance matrix localization method (IML) [5] and various wavelet transformation methods [1], [6]–[9]. Wavelet applications to electromagnetic integral equations were prompted by their success in numerical solutions of integral equations with nonoscillatory kernels [10]. The cited studies reported some sparsification of matrices, but only [1] studied the complexity of the MVM as the function of  $N$ . The study reported that matrix sparsification based on an

orthogonal wavelet transform produced sparse matrices with  $\beta N^2$  nonzero entries, where  $\beta < 1$ . This compares unfavorably with the FMM, AIM, and IML methods, all of which reduce the complexity of MVM to  $O(N^p)$  with  $p < 2$ .

This paper is concerned with the question whether discrete wavelet packets are able to reduce the cost of MVM in numerical solution of electromagnetic integral equations to  $O(N^p)$  with  $p < 2$ . The presentation assumes that initial impedance matrices are generated at the cost of  $O(N^2)$ . This is potentially a severe computational bottleneck that must be dealt with separately (see the conclusion section). The investigations are restricted to the electromagnetic scattering from two-dimensional (2-D) conducting cylinders with the combined field integral equation (CFIE) discretized by the method of moments. In the first section, we formulate the CFIE, discuss its discretization with pulse basis functions, and introduce the idea of sparsifying transformations. The next section briefly presents the matrix formulation of periodic Daubechies wavelet transform. Based on this construction, we discuss wavelet packets and present an adaptive algorithm for the selection of the near best basis transform. Numerical examples suggesting  $O(N^{4/3})$  sparsity of the transformed matrices and comparisons with other fast algorithms are given next. The last section contains conclusions and suggestions for future research.

## II. SPARSIFICATION

Consider the problem of computing the scattering of a  $\text{TM}(E_z)$  polarized electromagnetic wave from a 2-D conducting cylinder with the boundary contour  $C$ . The far-field scattering characteristics are obtained from the surface current  $J_z$  excited by an incident wave  $E_z^{\text{inc}}$ . In order to avoid problems with resonance the surface current is computed from the CFIE

$$\left(1 + \frac{\partial}{\partial n_x}\right) E_z^{\text{inc}}(\mathbf{x}) = \frac{\omega\mu_0}{4} \left(1 + \frac{\partial}{\partial n_x}\right) \int_C H_0^{(1)}(2\pi\lambda\mathbf{r}) J(\mathbf{x}') dl(\mathbf{x}') \quad (1)$$

where  $H_0^{(1)}$  is the zero-order Hankel function of the first kind,  $\mathbf{r} = |\mathbf{x} - \mathbf{x}'|$ ,  $\mathbf{x}, \mathbf{x}'$  denote points on  $C$ ,  $n_x$  is the outer unit normal at point  $\mathbf{x}$ , and  $\lambda$  is the excitation wavelength.

The integral equation is discretized in a standard way by subdividing contour  $C$  into  $N$  nonoverlapping contour pieces of (roughly) equal length and applying point matching (collocation) of pulse functions. In practical computations  $N$  is

Manuscript received November 26, 1996; revised May 23, 1997. This work was supported by grants from the University of Missouri Research Board and McDonnell Douglas Aerospace.

The author is with the Department of Mathematics and Computer Science, University of Missouri, St. Louis, MO 63121 USA.

Publisher Item Identifier S 0018-926X(98)03366-3.

proportional to the electric length of contour  $C$ . Discretization reduces the CFIE to the linear system

$$Zj = e \quad (2)$$

where  $Z$  is a full nonsymmetric complex nonsingular  $N \times N$  matrix.

Since the direct solution of the full system has a computational cost of  $O(N^3)$ , iterative methods must be used for large  $N$ . The cost of each iteration is dominated by a MVM, an  $O(N^2)$  operation for a dense matrix. The idea of sparsifying transformations is to find nonsingular matrices  $T_1$  and  $T_2$  so that the matrix  $Z' = T_1 Z T_2$  of the new system

$$Z'j' = e', \quad e' = T_1 e, \quad j = T_2 j' \quad (3)$$

has numerous very small elements which can be neglected (thresholded) without largely affecting the solution  $j'$ . Note that if  $T_2$  had a full set of eigenvectors as its columns and  $T_1 = T_2^{-1}$ , then  $Z'$  would be diagonal. Such a construction is obviously impractical because of its computational costs. Practical considerations require that matrices  $T_1, T_2$  must satisfy the following design criteria.

- 1) The matrix  $T_1 Z T_2$  must be (effectively) sparse.
- 2) Matrices  $T_1, T_2$  must be  $O(N)$  sparse, so that matrix-matrix multiplications cost only  $O(N^2)$ .
- 3) The condition number of  $Z'$  is not much larger than that of  $Z$ .

The last criterium is dictated by the fact that iterative methods converge more slowly for systems with larger condition numbers. Ideally, the transformation could *improve* the condition number serving as a preconditioner. Such transformations are difficult to construct. On the other hand, if both  $T_1$  and  $T_2$  are orthogonal, then the condition number of the new system is unchanged.

Recently [1], transformations based on Daubechies wavelets have been used to obtain sparsification of  $Z$ . The resulting transformation matrices were sparse, orthogonal, and produced considerable sparsity in  $Z'$ . However, for a fixed solution accuracy, the thresholded, wavelet-sparsified impedance matrices had  $O(N^2)$  nonzero elements, which seemed to disqualify the wavelet based approach in the future development of fast-solution algorithms. In next few sections, we describe a different algorithm (also using Daubechies wavelets), which considerably reduces computational complexity of the MVM's. The algorithm is based on the idea of discrete wavelet packets [11]) and is only slightly more expensive than the traditional wavelet transform.

### III. PERIODIC DAUBECHIES WAVELET TRANSFORM

In this section, we describe the discrete wavelet transform of vectors and matrices. In our considerations we use periodic Daubechies wavelets [12], but other wavelet constructions could be used as well. Given an integer  $p$ , we denote by  $\{h_k\}_1^{2p+2}$  the set of scaling coefficients. The corresponding wavelet coefficients are defined by  $g_k = (-1)^k h_{2p-k+3}$ . The

wavelets are said to have  $p$  vanishing moments if

$$\sum_{k=1}^{2p+1} g_k k^j = 0, \quad j = 0, \dots, p.$$

For a vector  $s^0$  of size  $N = 2^n$ , its periodic wavelet decomposition can be described in matrix notation by defining an  $N \times N$  matrix  $W_n$

$$W_n = \begin{bmatrix} H_n \\ G_n \end{bmatrix} \quad (4)$$

where  $H_n$  and  $G_n$  are matrices of size  $N/2 \times N$  called the low- and high-pass filters, respectively. For example, the low-pass filter  $H_n$  for the periodic Daubechies wavelets with one vanishing moment is given by

$$H_n = \begin{bmatrix} h_1 & h_2 & h_3 & h_4 & 0 & & \dots & 0 \\ 0 & 0 & h_1 & h_2 & h_3 & h_4 & 0 & \dots & 0 \\ & & & & & & \ddots & & \\ 0 & \dots & & & 0 & h_1 & h_2 & h_3 & h_4 \\ h_3 & h_4 & 0 & & & \dots & 0 & h_1 & h_2 \end{bmatrix}. \quad (5)$$

The high-pass filter  $G_n$  has the same structure as  $H_n$  but is defined in terms of wavelet coefficients  $g_k$ . The scaling and wavelet coefficients are defined in such a way that the matrix  $W_n$  is orthogonal [12].

The product  $W_n s^0$  is a decomposition of the vector  $s^0$  into the “average” vector  $s^1$  and the “difference” vector  $d^1$

$$W_n s^0 = [H_n s^0, G_n s^0]^t = [s^1, d^1]^t. \quad (6)$$

Continuing the process of recursive decomposition of “average” vectors  $s^j$ ,  $j = 1, \dots, l \leq n - \log_2 2p + 2 + 1$  one obtains the discrete wavelet transform (DWT) of the vector  $s^0$ . In matrix notation, the DWT is described by matrix  $T$  such that

$$T s^0 = W_{n-l} \cdots W_{n-1} W_n s^0 = [s^l, d^l, \dots, d^1]^t \quad (7)$$

where matrices  $W_{n-j}$  are block-diagonal matrices of the form

$$W_{n-j} = \begin{bmatrix} H_{n-j} \\ G_{n-j} \\ & I_{N-N/2^j} \end{bmatrix} \quad (8)$$

and  $I_{N-N/2^j}$  is the identity matrix of rank  $N - N/2^j$ . The discrete wavelet transform  $T$  is orthogonal ( $T$  is a product of orthogonal matrices). The reconstruction of vector  $s^0$  from its decomposition is obtained from

$$s^0 = T^t [s^l, d^l, \dots, d^1]^t. \quad (9)$$

Wavelet transformations of an arbitrary matrix  $A$  are effected by the product  $T A T^t$ . Note that the product  $T A$  results in the wavelet decomposition of columns of  $A$ . This is followed by the multiplication by  $T^t$  resulting in the wavelet decomposition of rows of  $T^t A$ .

Suppose that elements of  $s^0$  are the values of a smooth periodic function with the sampling rate proportional to  $N =$

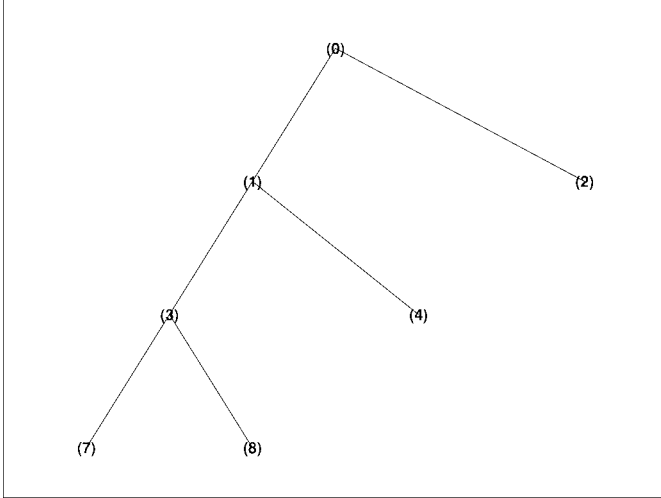


Fig. 1. Level 3 binary tree structure for the wavelet transform.

$2^n$ , for example,  $s^0(k) = \sin(2\pi k/2^n)$ ,  $k = 1, \dots, 2^n$ . Given  $p$ , such a vector  $s^0$  can be well approximated by

$$T^t [s^l, 0, \dots, 0]^t \quad (10)$$

for any sufficiently large  $N$ . Since  $l$  is proportional to  $n$ ,  $s^l$  has constant length, so  $s^0$  can be approximated by a short vector of constant size. This property have been used effectively in compression of matrices arising in discretization of integral operators with nonoscillatory kernels [10]. However, the situation changes when the elements of  $s^0$  come from an oscillatory function sampled with a fixed number of points per period. This occurs, for example, when  $s^0(k) = \sin(\pi k/8)$ ,  $k = 1, \dots, 2^n$ . For increasing  $N = 2^n$  it is necessary to retain an increasing number of high-pass sequences  $d^l$  to accurately compress  $S^0$  in this case. This is due to the spatial localization of the wavelets used. In such cases the windowed Fourier transform gives better compression. We will argue that the discrete wavelet packets (DWP) can be used to accommodate both cases. Thus, the DWP can be used in sparsification of matrices arising in discretization of integral equations of electromagnetics, especially in cases when the resolution of discretization is constant.

#### IV. WAVELET PACKET TRANSFORM

Returning to the decomposition of vector  $s^0$  into the low-pass component  $s^1$  and the high-pass component  $d^1$  we note that the DWT proceeds at the next step to decompose further only  $s^1$ . However, at this decomposition level two other approaches are possible. Either both  $s^1$  and  $d^1$  or only  $d^1$  (and not  $s^1$ ) can be decomposed. In matrix notation the first option gives

$$\begin{aligned} Ts^0 &= \begin{bmatrix} H_{n-1} \\ G_{n-1} \end{bmatrix} \begin{bmatrix} H_{n-1} \\ G_{n-1} \end{bmatrix} \begin{bmatrix} H_n \\ G_n \end{bmatrix} s^0 \\ &= \begin{bmatrix} H_{n-1} H_n s^0 \\ G_{n-1} H_n s^0 \\ H_{n-1} G_n s^0 \\ G_{n-1} G_n s^0 \end{bmatrix}. \end{aligned} \quad (11)$$

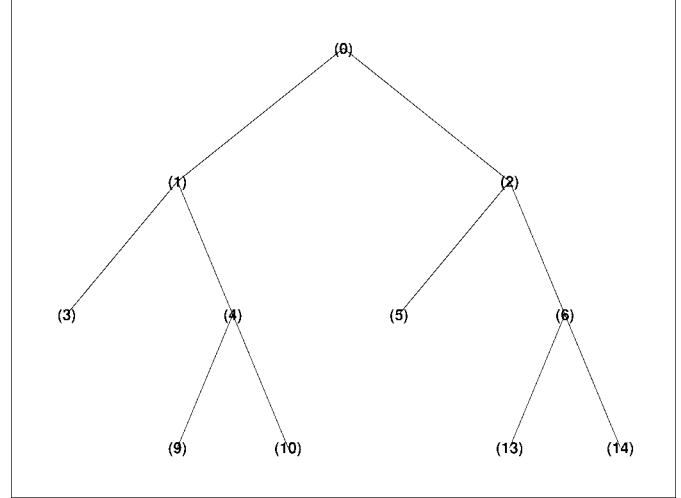


Fig. 2. Level 3 binary tree structure for a wavelet packet transform.

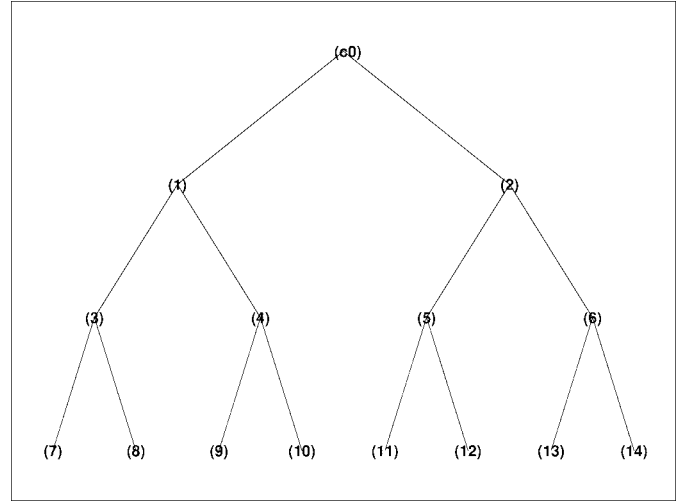


Fig. 3. Level 3 binary tree structure for the complete level decomposition transform.

The second approach results in the following description:

$$\begin{aligned} Ts^0 &= \begin{bmatrix} [I_{N/2}] & \\ & \begin{bmatrix} H_{n-1} \\ G_{n-1} \end{bmatrix} \end{bmatrix} \begin{bmatrix} H_n \\ G_n \end{bmatrix} s^0 \\ &= \begin{bmatrix} H_n s^0 \\ H_{n-1} G_n s^0 \\ G_{n-1} G_n s^0 \end{bmatrix}. \end{aligned} \quad (12)$$

Note that the transformation  $T$  in either case is orthogonal. If this process is repeated recursively with  $l$  levels it results in a binary tree structure of more than  $2^{2^l}$  possible decompositions of a vector. Figs. 1–3 present different decompositions of a vector with three levels of recursion: the wavelet transform, a wavelet packet, and the complete level transform.

The selection of the best basis from the wavelet packet should be made with respect to the maximum sparsity of the thresholded matrix for a prescribed solution error tolerance. This is a very difficult criterion to satisfy from both analytical and computational standpoints. The analytical difficulty lies in defining an appropriate information cost function (see [11]).

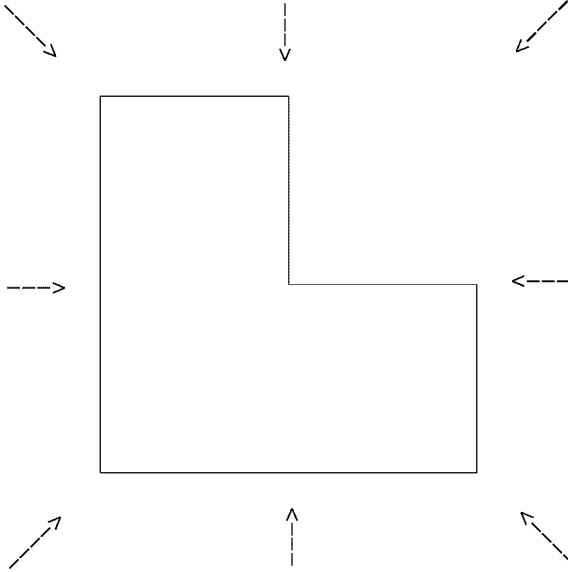


Fig. 4. Geometry of the L-shape contour and the incidence directions.

precisely related to the the error tolerance of the sparse system. The computational bottleneck stems from the fact that given any cost function, the best basis algorithm has complexity  $O(N \log(N))$  when applied to an  $N$  vector and  $O(N^2 \log(N))$  when applied to a square matrix.

However, it is possible to propose a viable  $O(N \log(N))$  best basis selection algorithm using an approach similar to that introduced in [9]. Starting with the incident wave vector  $e$  as the top node of the decomposition tree, a decision whether to continue decomposition at any given node is based on a comparison of norms of vectors at the parent and children nodes. The information cost function used as a criterion is

$$C(x) = \sum_i |x_i|, \quad x = [x_1, \dots, x_M]^t$$

where  $x$  is a vector of decomposition coefficients related to the node, and  $M = 2^r$  for some positive integer  $r$ . If the norm of the parent node vector is smaller than the norm of its two children, that part of the tree is not decomposed further. It is easily observed that if the initial data is of length  $N$ , the selection algorithm stops after  $O(N \log(N))$  operations.

Once the tree structure has been determined, the orthogonal transformation  $T$  is known and it is applied to matrix  $Z$  to obtain  $Z' = TZT^t$ . The transformed matrix  $Z'$  is then thresholded and the resulting system solved for an approximation of the solution vector  $j'$ .

The above adaptive construction of the transformation matrix  $T$  can be extended to problems with many excitation vectors (in the case of RCS computations). Given a block of  $m$  column vectors  $E = [e^1, \dots, e^m]$ , the adaptive algorithm decomposes  $E$  instead of a single  $e_i$  using a modified information cost function

$$C(x) = \sum_j \sum_i |x_i^{(j)}|, \quad x = \begin{bmatrix} x_1^{(1)} & \dots & x_1^{(m)} \\ \vdots & & \vdots \\ x_M^{(1)} & \dots & x_M^{(m)} \end{bmatrix}.$$

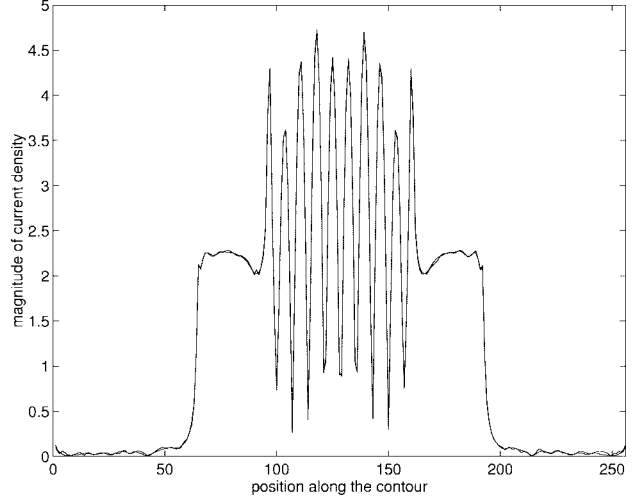


Fig. 5. Magnitude of the surface current density along the L-shaped contour induced by a plane wave incident at  $45^\circ$  into the concave corner. The scatterer has length  $25.6\lambda$  and is discretized with  $N = 256$ .

The cost of the tree selection changes to  $O(mN \log(N))$ . In the next section, the adaptive wavelet packet algorithm with a block of incidence vectors with evenly spaced angles is applied to scattering from two cylinders.

## V. MATRIX SPARSITY—NUMERICAL EXAMPLES

In this section, the results of a study of matrix sparsity as a function of the problem size are presented. Scattering of plane waves from 2-D cylinders is computed numerically using a constant number of test functions per wavelength. The surface currents induced on a 2-D conducting cylinder by planar waves are described by the integral equation (1). The incident waves are given by

$$E_z^{\text{inc}}(\mathbf{x}) = \exp(i\mathbf{k} \cdot \mathbf{x}), \quad \mathbf{k} = 2\pi\mathbf{d}/\lambda \quad (13)$$

where  $\mathbf{d}$  is the incidence direction unit vector. Two different cylinder contours were considered: a circle and an L-shape (see Fig. 4 for the geometry of the latter contour). Equation (1) was discretized with pulse functions and point matching. The support of pulse functions was  $\lambda/10$  throughout all experiments. For both contours, we computed the scattering for increasing incident frequency (or equivalently, for the increasing electrical cylinder size), adjusting the threshold level  $\tau$  to maintain the relative residual error  $\|e' - Z' j'_{\text{comp}}\|/\|e'\|$  of  $(1 \pm 0.01)\%$ , where  $j'_{\text{comp}}$  is the solution computed using the thresholded sparse matrix  $Z'$ . This level of solution accuracy produces approximate solutions visually indistinguishable from those obtained from the full systems. We noted that  $\tau$  had to be decreased as the problem size grew to maintain the accuracy of the solution of the sparse system. Fig. 5 shows the magnitude of the current density along the perimeter of the L-shape domain induced by the planar wave incident at  $45^\circ$  (i.e., into the concave corner of the contour). Here the perimeter length is  $25.6\lambda$  and the current was computed with the dense and the sparse matrices. The curves practically overlap.

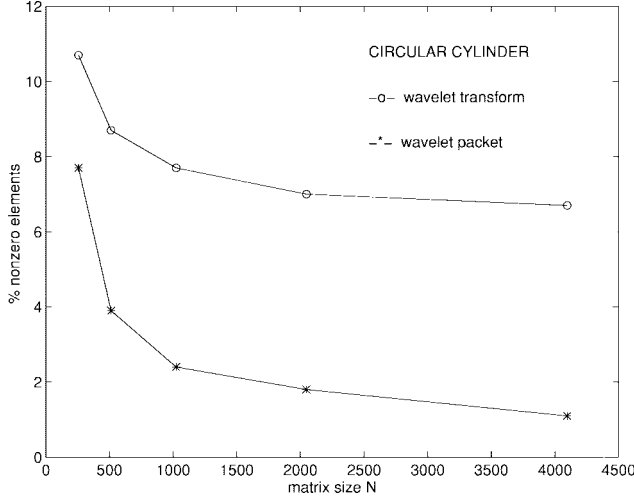


Fig. 6. DW and DWP matrix sparsity as a function of size  $N$  for the circular cylinder. Periodic Daubechies wavelets with eight vanishing moments used. Threshold levels adjusted to maintain relative errors of  $(1 \pm 0.01)\%$ .

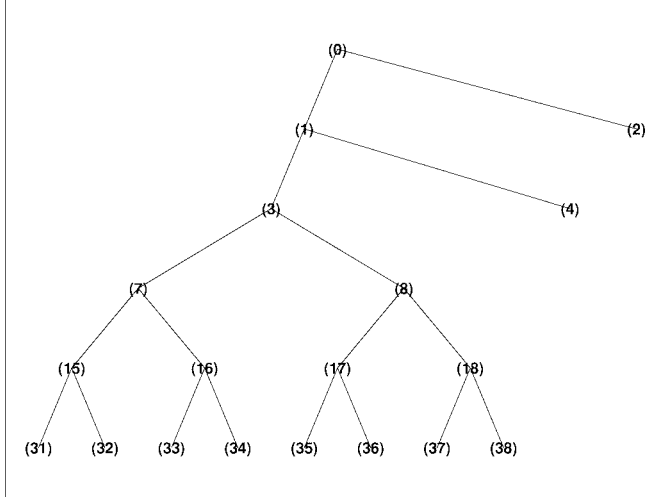


Fig. 7. Tree structure for the L-shaped domain  $N = 512$ .

The system sizes studied ranged from  $N = 256$  (contour length of  $25.6\lambda$ ) to  $N = 4096$  (contour length of  $409.6\lambda$ ). The sparsity results for the circular cylinder are presented in Fig. 6. The wavelet packet tree was computed from a single planar incident wave. It can be seen that the DWP produces much higher sparsity than does the DWT. Moreover, the sparsity of DWP transformed matrices does not level off for large  $N$ , but continues to decrease. Specifically, for the circular cylinder the DWT produced the sparsities ranging from 10.7% for  $N = 256$  to 6.7% for  $N = 4096$ . The sparsities obtained from the DWP ranged from 7.4% for  $N = 256$  to 1.1% for  $N = 4096$ .

Similar results were obtained for the L-shaped contour. In this case, the wavelet packet tree for the L-shaped contour was computed from a block of eight right-hand side vectors obtained from planar waves with different incident angles as shown in Fig. 4. This was done to show that the DWP produces good sparsification with many different excitation

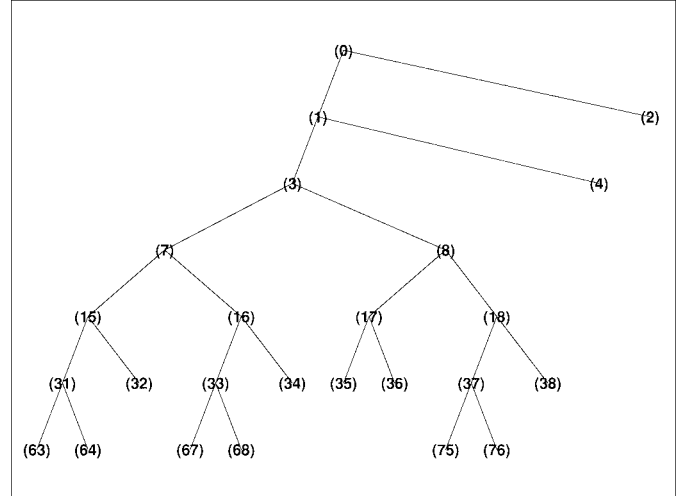


Fig. 8. Tree structure for the L-shaped domain  $N = 1024$ .

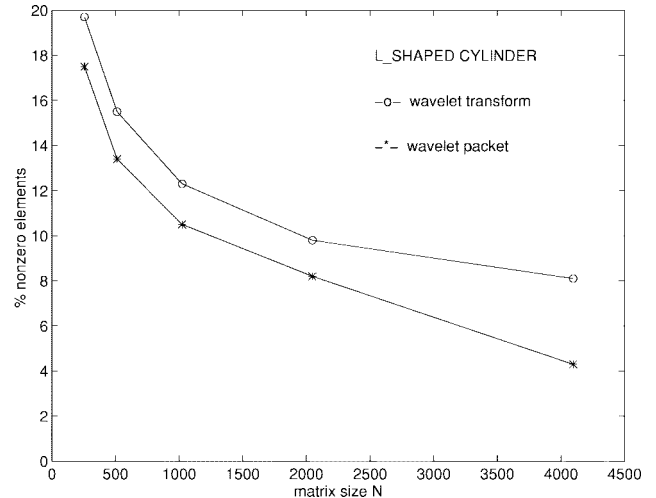


Fig. 9. DW and DWP matrix sparsity as a function of size  $N$  for the L-shaped cylinder. Periodic Daubechies wavelets with eight vanishing moments used. Threshold levels adjusted to maintain relative errors of  $(1 \pm 0.01)\%$ .

vectors. Figs. 7 and 8 give the tree diagrams for the basis selection in case of  $N = 512$  and  $N = 1024$ . Note that first two levels of decomposition in both cases are identical to the standard DWT. The additional sparsity obtained in DWP comes from decomposition at levels  $l > 2$ . Since all excitations vectors play a role in the construction of the wavelet packet tree, the tree construction is based more on the geometry of the scatterer and less on the relation between the excitation and solution vectors.

The DWT and DWP sparsity results for the L-shaped cylinder are presented in Fig. 9. As in the case of the circle, the DWP produces higher sparsity than the DWT and the DWP-produced sparsity changes faster as the problem scales. Specifically, the DWT sparsities range from 20.3% for  $N = 256$  to 8.3% for  $N = 4096$ . The sparsities obtained from the DWP ranged from 17.7% for  $N = 256$  to 4.2% for  $N = 4096$ . Since the relative importance of the contour corners diminishes with the increase of  $N$ , the sparsities will eventually approach

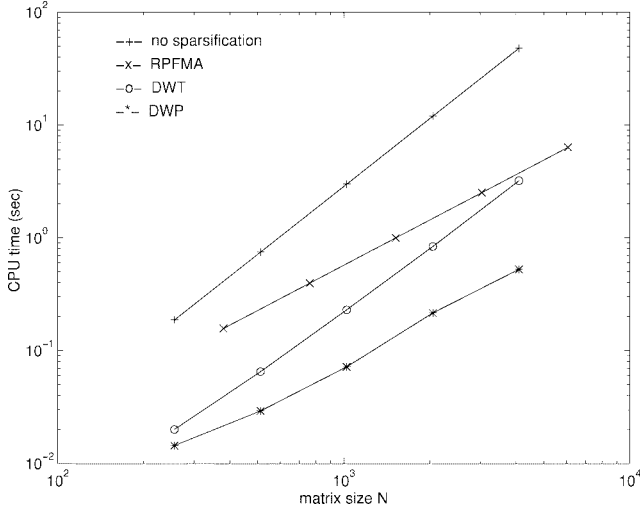


Fig. 10. CPU times for one matrix–vector multiplication as a function of size  $N$  for a circular cylinder.

those of the circular cylinder. This means that DWT-produced sparsities will level off (as suggested in [1]), whereas the percentage of nonzero elements in DWP-based matrices will continue to decrease.

Fig. 10 compares the CPU times required for a single MVM as a function  $N$  using the DWP, DWT, and the ray propagation fast-multipole algorithm (RPFMA) [3]. The RPFMA was shown to reduce MVM time to  $O(N^{4/3})$  (for constant relative residual error). The times for RPFMA and DWT were obtained from [1] and refer to computations on a SUNSPARC10 workstation. The DWP and DWT algorithms were coded in MATLAB and run on a SUNSPARC1000. To make the comparison it was necessary to scale the DWP CPU times. Since the CPU time for one MVM is proportional to the number of nonzero matrix elements, the times for DWP algorithm were computed by scaling the DWT times by the ratio of sparsities of DWP and DWT matrices. As it was observed in [1] the slope for the DWT algorithm is roughly the same to that for computations with dense matrices indicating that DWT is a  $O(N^2)$  method. The RPFMA-based matrix–vector multiply is slower than the DWT-based multiply for small  $N$ , but for  $N > 5000$  it will always be faster due to its  $O(N^{4/3})$  complexity. The DWP-based matrix–vector multiply is fastest of all—the complexity seems to grow at about the same rate as for the RPFMA algorithm, but with a much smaller leading constant. Fig. 11 shows that the number of nonzero elements in impedance matrices for circular and L-shaped cylinders sparsified by the DWP algorithm is roughly of order  $O(N^{4/3})$  (the slopes are nearly parallel to a line with slope 4/3).

It is important to emphasize that a comparison of CPU times for a single MVM can not be used as a sole indicator of the competitiveness of a method. Other factors such as the cost of generating of initial matrix, the cost of matrix transformations, or the number of iterations required for convergence need to be taken into the account. Some of these issues we discuss in the following section. However, the comparisons given here indicate that if these obstacles are overcome the DWP

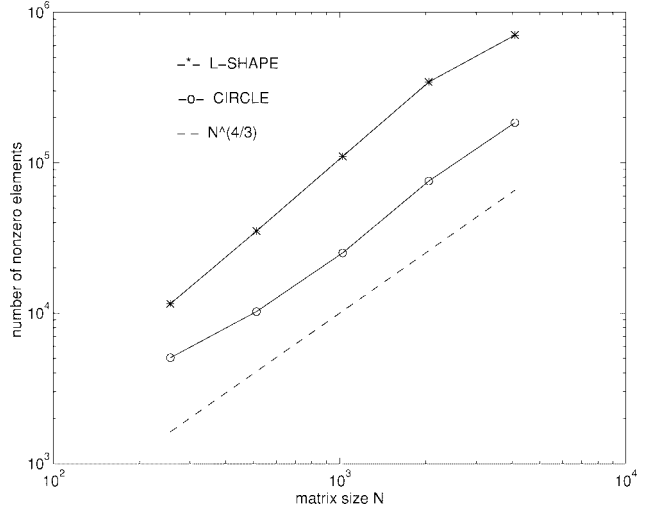


Fig. 11. Number of nonzero elements as a function of size  $N$  for circular and L-shaped cylinders; DWP sparsification. Threshold levels adjusted to maintain relative errors of  $(1 \pm 0.01)\%$ .

transformations could be developed into an attractive and practical technique.

## VI. CONCLUSIONS

In this paper, we described an application of the DWP transformations, which reduce the complexity of matrix–vector multiplications in iterative solutions of discretized 2-D CFIE roughly equal to  $O(N^{4/3})$ . This reduction of complexity is obtained assuming a fixed number of basis functions per incident wavelength. The order of the complexity is similar to that of the RPFMA method, but the DWP-based matrix–vector multiplication is much faster due to a smaller complexity constant.

Many of the ideas presented here need further development, most notably the problems of generating the initial matrix in less than  $O(N^2)$  time and the extension of the DWP approach to three-dimensional (3-D) surfaces. It is possible to overcome the first problem by initially grouping the basis functions and representing the group interactions via some approximations. This approach is very much as the one in the FMM method and results in an approximation to the dense matrix in  $O(N^p)$ ,  $p < 2$  operations. This can be followed by DWP transformations of each of the blocks representing interactions between two groups resulting in further sparsity of the global matrix. It can be shown that a matrix represented by  $O(N^p)$ ,  $p < 2$  elements can be DWP transformed in  $O(N^p \log(N))$ ,  $p < 2$  time. This extra cost can be offset by a higher sparsity of the transformed matrix.

Clearly, in the block setting the periodic wavelets should not be used for construction of DWP trees since none of the blocks correspond to a periodic surface structure. However, there exist wavelets defined on intervals [13], which seem to be well suited for the task. The interval wavelets may also be used in extending the DWP approach to 3-D surfaces. Here, as in two dimensions, the block approximations will produce an approximation of the initial matrix in less than  $O(N^2)$  time and the block DWP is used to produce further sparsity. If a

block represents interactions of basis functions supported on a rough part of the surface, the DWP is simply not be applied to that block.

In summary, the above-described use of discrete wavelet packet transformations for the solution of electromagnetic integral equations appears to reduce the computational complexity of matrix–vector multiplications. Its further development (possibly in conjunction with other fast methods) may contribute to the improvement of the existing fast codes.

#### ACKNOWLEDGMENT

The author would like to thank Dr. L. N. Medgyesi-Mitchang and Dr. D. S. Wang for introducing the problem, Prof. G. V. Welland for suggesting the use of wavelet packets, and all three of them for many fruitful discussions on fast solvers for CEM.

#### REFERENCES

- [1] R. L. Wagner and W. C. Chew, "A study of wavelets for the solution of electromagnetic integral equations," *IEEE Trans. Antennas Propagat.*, vol. 43, pp. 802–810, Aug. 1995.
- [2] V. Rokhlin, "Rapid solution of integral equations of scattering theory in two dimensions," *J. Comp. Phys.*, vol. 86, no. 2, pp. 414–439, 1990.
- [3] R. L. Wagner and W. C. Chew, "A ray-propagation fast multipole algorithm," *Microwave Opt. Technol. Lett.*, vol. 7, no. 10, pp. 435–438, 1994.
- [4] E. Bleszynski, M. Bleszynski, and T. Jaroszewicz, "Fast integral-equation solver for electromagnetic scattering problems," in *IEEE AP-S Int. Symp. Dig.*, Seattle, WA, June 1994, pp. 416–419.
- [5] F. X. Canning, "Sparse approximations for solving integral equations with oscillatory kernels," *SIAM J. Sci. Statist. Comput.*, vol. 13, no. 1, pp. 71–87, 1992.
- [6] D. S. Wang and G. Welland, "Modeling of electromagnetic scattering using wavelet techniques for geometry modeling and expansion functions," in *URSI Radio Sci. Meet. Dig.*, Detroit, MI, June 1992, p. 277.
- [7] H. Kim and H. Ling, "On the application of fast wavelet transform to integral equation solution of electromagnetic scattering problems," *Microwave Opt. Technol. Lett.*, vol. 6, no. 3, pp. 168–173, 1993.
- [8] G. Wang, "A hybrid wavelet expansion and boundary element analysis of electromagnetic scattering from conducting objects," *IEEE Trans. Antennas Propagat.*, vol. 43, pp. 170–178, Feb. 1995.
- [9] Z. Baharav and Y. Levitan, "Impedance matrix compression using adaptively constructed basis functions," *IEEE Trans. Antennas Propagat.*, vol. 44, pp. 1231–1238, Sept. 1996.
- [10] G. Beylkin, R. Coifman, and V. Rokhlin, "Fast wavelet transforms and numerical algorithms i," *Commun. Pure Appl. Math.*, vol. XLIV, pp. 141–183, 1991.
- [11] M. V. Wickerhauser, *Adapted Wavelet Analysis from Theory to Software*. Boston, MA: A. K. Peters, 1994.
- [12] I. Daubechies, "Ten lectures on wavelets," CBMS Lecture Notes, SIAM, Philadelphia PA, vol. 61, 1992.
- [13] A. Cohen, I. Daubechies, and P. Vial, "Wavelets on the interval and fast wavelet transforms," *Appl. Computat. Harmonic Anal.*, vol. 1, no. 1, pp. 54–81, 1993.



**Wojciech L. Golik** received the M.Sc. degree in mechanical engineering from Poznan Technical University, Poznan, Poland, in 1982, and the M.Sc. and Ph.D. degrees in mathematics from New Mexico State University, Las Cruces, in 1985 and 1989, respectively.

Since 1988, he has been with the Department of Mathematics and Computer Science, University of Missouri, St. Louis. His research interests include numerical differential equations, computational electromagnetics, and numerical linear algebra.